Molecular Emission from G345.01+1.79

S.V. Salii[1], A.M. Sobolev[1], N.D. Kalinina[1] S.P. Ellingsen[2], D.M. Cragg[3], P.D. Godfrey[3], P. Harjunpää[4], I.I. Zinchenko[5]

[1]Astronomical Observatory of Ural State University
620083, Ekaterinburg, Lenin str. 51, Russia
E-mail: Svetlana.Salii@usu.ru, Andrej.Sobolev@usu.ru
[2]University of Tasmania, Hobart, Australia
[3]Monash University, Clayton, Australia
[4]Helsinki University, Helsinki, Finland
[5]Institute of Applied Physics, N.Novgorod, Russia

Abstract

We present SEST observations of G345.01+1.79 in maser and 'quasi-thermal' lines of CH_3OH, lines of SiO, CS and some other shock tracing molecules. For the first time weak methanol maser emission was detected at frequencies 165.05 and 165.06 GHz. The observed 'quasi-thermal' CH_3OH and SiO (2-1) lines display pronounced blue wings confined to the G345.01+1.79(S) position. Velocities of CH_3OH and OH maser features lie well within the wing. So, there is a high probability that interaction of the wind from the young star with ambient material is responsible for the creation of masers and production of the blue non-gaussian wing. Comparison of velocities for 'quasi-thermal' and maser lines shows that the bow shock velocity relative to the bulk of cloud material is about 10 kms^{-1}. So, most probably we are dealing with the first clear example of an ultracompact HII region moving through a molecular cloud. Modelling of CH_3OH 'quasi-thermal' emission and consideration of maser profiles shows that the cloud material is greatly inhomogeneous.
Keywords: *stars: formation – ISM: clouds – ISM: molecules – radio lines*

1. Introduction

The southern molecular cloud G345.01+1.79 (hereafter G345) shows various signs of interaction of young massive stars with their environment.

G345 displays strong emission in methanol (CH_3OH), hydroxyl (OH) and water vapor (H_2O) maser transitions (Caswell et al., 1995b; Caswell & Haynes, 1983; Caswell et al., 1983; Braz & Epchtein, 1983). VLBI observations have shown that the source contains 2 Class II CH_3OH maser sites, G345(S) and G345(N), according to Norris et al. (1993) notation. Positions of OH masers

coincide with those of CH_3OH masers in G345(S) (Caswell, 1997; Caswell et al., 1995b). H_2O masers in G345 are situated apart from IRAS point source and near infrared sources (NIR) (Testi et al., 1994). They presumably correspond to the sites containing young stellar objects (YSO) at the stages preceding formation of ultracompact HII regions (UCHII)(Cesaroni et al., 1997). Observations by Testi et al. (1994) have shown that the G345(S) OH maser site is situated at the edge of a strong NIR source coincident in position with IRAS16533-4009. Infrared spectrum obtained by Volk et al. (1991) indicates that this source is an UCHII. Interferometry by Caswell (1997) places CH_3OH and OH masers in G345(S) on the western side of UCHII radio continuum image.

2. Observations

The observations were made in October 1997 and March 1999 with the SEST(Swedish-ESO Submillimetre Telescope, La Silla, Chile). The molecular cloud was mapped in SiO(2-1), CH_3OH $5_K - 4_K$ and $C^{34}S$(5-4) lines. Altogether 54 positions were observed with a $20''$ spacing. Direction ($\alpha_{1950.0} = 16^h53^m19.7^s$, $\delta_{1950.0} = -40°09'46''$) toward the methanol maser cluster G345(S) was chosen as a map center. A number of additional lines were observed toward this position. Full list of observed lines includes 32 lines of CH_3OH and the lines of SiO, HCN, HCO^+, DCN, $C^{34}S$, $C^{33}S$, $C^{18}O$, ^{13}CO, H_2S, and SO at frequencies around 80, 86, 88, 96, 110 156, 165, 216 and 241 GHz.

3. SiO

The SiO(2-1) and (5-4) lines peak at V_{LSR} about –15 kms^{-1}. They exhibit asymmetric wing emission extending from about –50 kms^{-1} on the blue-shifted side to +10 kms^{-1} on the red-shifted side. In the SiO(5-4) spectrum the blue wing is more pronounced while the intensity of this line is lower. The SiO(2-1) spectrum towards the map center is shown in Fig.1.

Velocity channel maps for the SiO(2-1) emission over the range –50→ 10 kms^{-1} are shown in Fig.2. The wing emission in four ranges corresponding to high-velocity and low-velocity blue-shifted wings ($-50 \rightarrow -25$ kms^{-1} and $-25 \rightarrow -18$ kms^{-1}, respectively), and low- and high-velocity red-shifted wings ($-12 \rightarrow -8$ kms^{-1} and $-8 \rightarrow 10$ kms^{-1}, respectively) are shown as contour maps. The distribution of the line core emission ($-18 \rightarrow -12$ kms^{-1}) is shown as a grey scale image in each panel.

SiO emission from the quiescent gas ($-18 \rightarrow -12$ kms^{-1}) peaks near the

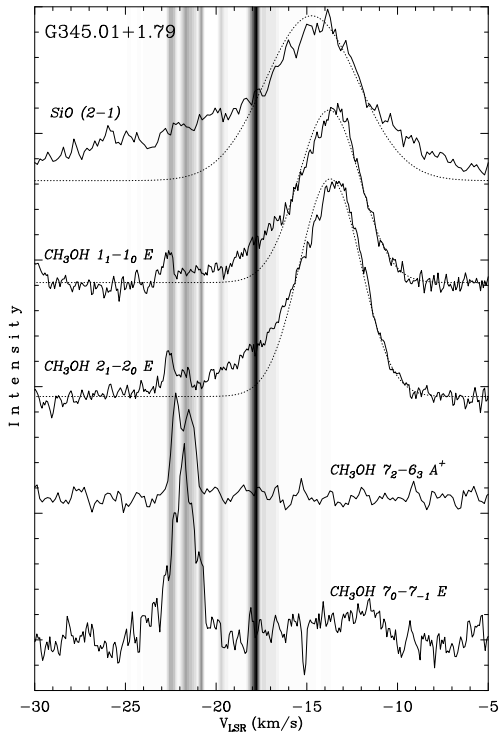

Figure 1: Non-gaussian wings in the spectra of SiO (2-1) and CH_3OH quasi-thermal lines and weak CH_3OH maser lines toward G345(S). Intensity of SiO (2-1) line is 0.6 K, intensities of the CH_3OH lines are listed in the table. Spectrum of the CH_3OH $5_1 - 6_0$ A^+ maser line is shown by shades of grey

methanol maser cluster G345(N). The low-velocity wing emission ($-25 \rightarrow -18$ and $-12 \rightarrow -8\,\mathrm{kms}^{-1}$) is extended. The emission in the low-velocity blue wing is more extended and the intensity maximum is located $10''$ west of G345(N), while emission in the low-velocity red wing peaks $30''$ east of G345(N).

The high-velocity blue-shifted wing emission ($-50 \rightarrow -25\,\mathrm{kms}^{-1}$) is clearly concentrated to the western side of the map and the intensity maximum lies at $(20'', 20'')$, i.e., about $30''$ west of G345(N). Weak high-velocity red-shifted emission ($-8 \rightarrow 10\,\mathrm{kms}^{-1}$) arises predominantly east of G345(N). Separate blue- and red-shifted high-velocity wing emission regions suggest the presence of a bipolar molecular outflow. Its central source is probably located near G345(N) and its projected position angle in the plane of the sky is close to 90°.

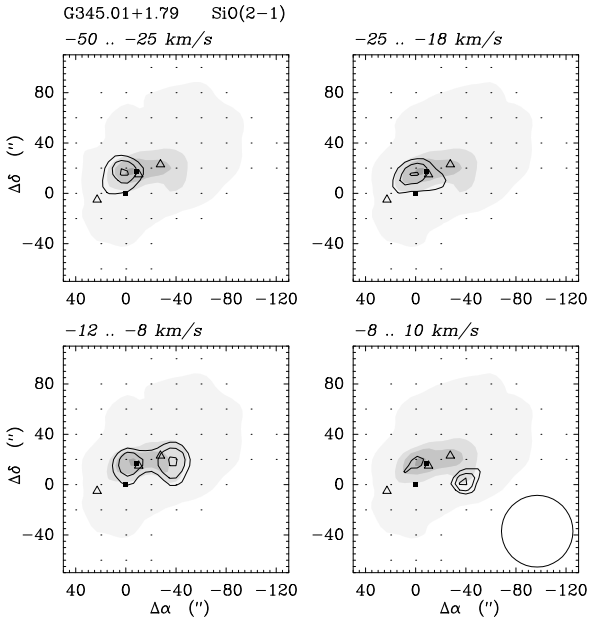

Figure 2: Channel maps of the SiO line wing emission (contours) superimposed on the line core emission (grey scale). The locations of 6.7 GHz methanol maser sites G345(S) and G345(N) are marked by filled squares, and locations of H_2O masers (Caswell et al., 1983) are marked by open triangles. The half power beam size is shown in the lower right panel

4. Methanol

Distribution of methanol emission in G345 resembles that of SiO. However, CH_3OH lines are considerably narrower indicating that turbulent motions are more developed in SiO abundant regions.

CH_3OH lines manifest strong and extended non-gaussian wings (see Fig.1). The blue wing is most pronounced at the map center. Noteworthy that velocities of components of the brightest CH_3OH maser ($5_1 - 6_0$ A^+ at 6.7 GHz) toward G345(S) correspond to velocities of the blue wing of the CH_3OH and SiO lines (Fig.1).

One remarkable feature of the G345(S) maser site is that the maser spots show clear increase in V_{LSR} with the distance from the center of UCHII (Norris et al., 1993). Such a velocity pattern corresponds well to the motions of matter in the wake of the bow shock produced by the movement of UCHII ionizing star toward the observer (Van Buren et al., 1990; Raga et al., 1997).

Other feature of G345(S) is that maser spots show dramatic increase in the ratio of fluxes of 6 GHz and 12 GHz methanol maser lines (hereafter F6 and F12, respectively) with the distance from UCHII center. Indeed, comparison

Table 1 CH_3OH weak maser components of molecular cloud G345.01+1.79

Frequency MHz	Transition	Area $Kkms^{-1}$	V_{LSR} kms^{-1}	ΔV_{LSR} kms^{-1}	T_A^* K
86903.06	$7_2 - 6_3 A^+$	0.46(0.02)	-21.82(0.03)	1.33(0.06)	0.33
156488.95	$8_0 - 8_{-1} E$	4.33(0.13)	-19.08(0.10)	3.33(0.22)	1.22
156602.42	$2_1 - 3_0 A^+$	1.32(0.13)	-20.62(0.10)	2.56(0.27)	0.49
156828.51	$7_0 - 7_{-1} E$	3.06(0.07)	-21.78(0.02)	1.76(0.05)	1.66
157048.62	$6_0 - 6_{-1} E$	3.98(0.12)	-21.11(0.05)	2.96(0.11)	1.27
157178.97	$5_0 - 5_{-1} E$	4.72(0.13)	-21.24(0.04)	2.88(0.10)	1.54
157246.10	$4_0 - 4_{-1} E$	3.82(0.12)	-21.73(0.04)	2.99(0.13)	1.20
165050.19	$1_1 - 1_0 E$	0.06(0.01)	-22.64(0.06)	0.60(0.14)	0.09
165061.16	$2_1 - 2_0 E$	0.12(0.02)	-22.46(0.09)	1.12(0.23)	0.10
216945.60	$5_1 - 4_2$ E	0.27(0.14)	-20.45(0.92)	3.29(1.57)	0.08

with spectra from Caswell et al. (1995a,b) show that F6/F12 is about 0.35 for the –23.8 kms^{-1} feature and increases to more than 150 for the –18 kms^{-1} feature.

From the point of view of Class II CH_3OH maser modelling given in Sobolev et al. (1997a,b) such an F6/F12 behavior for the bright maser spots can be explained by the increase of UCHII emission dilution, decrease in hydrogen number density and increase of maser beaming with the distance from UCHII center. Increase of dilution of UCHII emission with offset is straightforward. However, the difference in F6/F12 is too big to be explained by this effect alone. So, we think that the phenomenon is borne by combined action of mentioned factors. This is likely to take place since the increase of offset from the head of bow shock is followed by 1) increasing CH_3OH column density of less dense material and 2) increasing ratio of radial to tangential dimensions of emitting region which brings higher beaming.

In order to elucidate the situation with weaker Class II CH_3OH masers in G345(S) we performed observations of methanol maser candidates.

In the 10 lines listed in the table we detected components with velocities –24 – –20 kms^{-1} which are about 10 kms^{-1} lower than velocities of the quasi-thermal methanol lines. At the same time they show good agreement with velocities of maser features observed in Class II maser lines (Fig.1). The lines are narrow and we believe that they are really masers despite their quite low intensities. Our observations borne clear detection of new weak methanol masers at 165.05 and 165.06 GHz and marginal detection of maser at 216.9 GHz.

Maser modelling presented in Sobolev et al. (1997b) shows that different maser lines may form in different regimes. This is in accordance with our observations displaying noticeable difference in the line profiles shown in Fig.1.

Thus, observations of weaker methanol maser lines indicate that the physical conditions in G345(S) maser formation region are strongly inhomogeneous.

5. Non-LTE modelling of methanol emission

The LVG modelling of methanol emission at map center position provides much better fit than the rotational diagram (see Fig.3) indicating that excitation of methanol lines in this object exhibits great departures from LTE. Moreover, considerations of the previous sections provide evidence that molecular material in G345 is greatly inhomogeneous.

So, we dared to make a step further in order to investigate possible variation of parameters of cloud constituents. In order to do that we applied 2-component LVG modelling of quasi-thermal emission in methanol lines. Fig. 3 clearly shows that the 2-component modelling provides much better fit to observational data. Results of this modelling demonstrate inhomogeneity of molecular material in G345 and will be described in a separate paper.

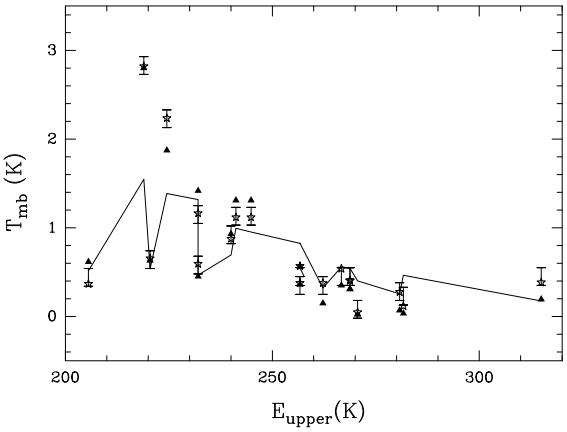

Figure 3: Results of LVG modelling of emission in 'quasi-thermal' methanol lines from map center position. Error bars show observed intensities; solid line connects intensities of rotational diagram; triangles show intensities of the best 1-component LVG fit and stars show intensities from 2-component LVG modelling

6. Conclusions

The G345.01+1.79 cloud was observed in a number of molecular lines. For the first time a weak methanol maser emission in the lines at 165.05 and 165.06 GHz was detected. Maser component in the 216.94 GHz line was marginally detected.

Presence of extended emission of shock tracing molecules shows that the molecular material in the cloud is greatly affected by the passage of shock waves.

Analysis of SiO line emission indicates possible presence of an outflow.

Consideration of the data on methanol and hydroxyl masers in G345(S) maser site suggests that these masers are formed in the region affected by the passage of bow shock borne by interaction of the wind from the young star moving toward the observer with material of the bulk of the G345 cloud. This hypothesis explains observed maser spectra and velocity pattern of maser spots.

LVG modelling of methanol line emission and consideration of methanol maser line profiles show that the molecular material in G345 is greatly inhomogeneous.

Acknowledgements

Studies were supported by INTAS, RFBR and ARC.

References

Braz, M.A., Epchtein, N. 1983, A&AS 54, 167
Caswell, J.L., 1997, MNRAS 289, 203
Caswell, J.L., Batchelor, R.A., Forster, J.R., Wellington, K.J., 1983, Austral.J.Phys. 36, 401
Caswell, J.L., Haynes R.F., 1983, Austral.J.Phys. 36, 361
Caswell, J.L., Vaile, R.A., Ellingsen, S.P., Norris, R.P., 1995a, MNRAS 274, 1126
Caswell, J.L., Vaile, R.A., Ellingsen, S.P., et al., 1995b, MNRAS 272, 96
Cesaroni, R., Felli, M., Testi, L., et al., 1997, A&A 325, 725
Norris, R.P., Whiteoak, J.B., Caswell, J.L., et al., 1993, MNRAS 412, 222
Raga, A.C., Mellema, G., Lundqvist, P., 1997, ApJS 109, 517
Sobolev, A.M., Cragg, D.M., Godfrey, P.D., 1997a, A&A 324, 211
Sobolev, A.M., Cragg, D.M., Godfrey, P.D., 1997b, MNRAS 288, L39
Testi, L., Felli, M., Persi, P., Roth, M., 1994, A&A 288, 634
Van Buren, D., MacLow, M.M., Wood, D.O.S., Churchwell E., 1990, ApJ 353, 570
Volk, K., Kwok, S., Stencel, R.E., Brugel, E., 1991, ApJS 77, 607